We are IntechOpen,
the world's leading publisher of
Open Access books
Built by scientists, for scientists

6,900
Open access books available

185,000
International authors and editors

200M
Downloads

154
Countries delivered to

Our authors are among the

TOP 1%
most cited scientists

12.2%
Contributors from top 500 universities

CLARIVATE ANALYTICS
BOOK CITATION INDEX
INDEXED

WEB OF SCIENCE™

Selection of our books indexed in the Book Citation Index
in Web of Science™ Core Collection (BKCI)

Interested in publishing with us?
Contact book.department@intechopen.com

Numbers displayed above are based on latest data collected.
For more information visit www.intechopen.com

6

Formation of Oxide Nanowires by Thermal Evaporation and Their Application to Gas Sensors

Toshinari Yamazaki
Graduate School of Science and Engineering,
University of Toyama, Toyama
Japan

1. Introduction

Oxide semiconductor gas sensors are based on their change in resistance upon exposure to oxidizing or reducing gases. While gas sensors made of conventional particles and thin films of oxide semiconductors have been studied for these several tens of years, gas sensors made of nanowires have been studied for these ten years because they have possibility of indicating excellent gas sensing properties, owing to the discriminating structure of the nanowires. The high surface-to-volume ratio of the nanowires is expected to provide high sensitivity. The one dimensionally long shape of the nanowires may lead to favourable sensing properties. There are two types of nanowire sensor. One is made of nanowires dispersed on a substrate equipped with a pair of electrodes while the other is made of a single nanowire. In our study, the former type was investigated.

We have first developed three types of evaporation method for forming oxide nanowires and then investigated their structure. The first one is a conventional vapour transport method. The second one is simple evaporation in ambient atmosphere. The last one is a method using a conventional vacuum evaporator with its chamber filled with prescribed pressure of oxidizing gas such as ambient air; we call this method a modified gas evaporation method.

To clarify the feature of nanowire sensors, we have investigated the properties of the gas sensors made of nanowires. The effect of Pd doping was examined in the sensors made of SnO_2 nanowires formed by the vapour transport method, and their performance was compared with sputtered film sensor. It is of great interest to investigate the effect of the thickness and length of the nanowires. The effect of the thickness was investigated for WO_3 nanowires formed by the vapour transport method and SnO_2 nanowires formed by the modified gas evaporation method, while the effect of the length was investigated for the SnO_2 nanowires formed by the modified gas evaporation method in comparison with the gap lengths of electrodes. Gas sensors made of Ga_2O_3 and TeO_2 nanowires, which have been rarely studied, were also investigated for exploring new nanowire sensor materials. In this article, the methods for forming nanowires are first explained, and then the structure of the nanowires and gas sensing properties are introduced.

2. Methods for forming nanowires

2.1 Vapor transport method

In the conventional vapor transport method, which is shown in Fig. 1(a), an alumina boat loaded with a raw material was placed in a quartz tube inserted into a horizontal electric furnace, and Ar gas was introduced through the quartz tube. Although oxygen gas was not introduced, oxide nanowires were obtained probably because of unintentional introduction of a minute amount of oxygen gas. This method was used for the formation of SnO_2 (Shen et al.,2009), WO_3, and Ga_2O_3 (Liu et al., 2008) nanowires, where the position of the substrate, the flow rate and pressure of Ar, and the furnace temperature was adjusted, depending on the materials.
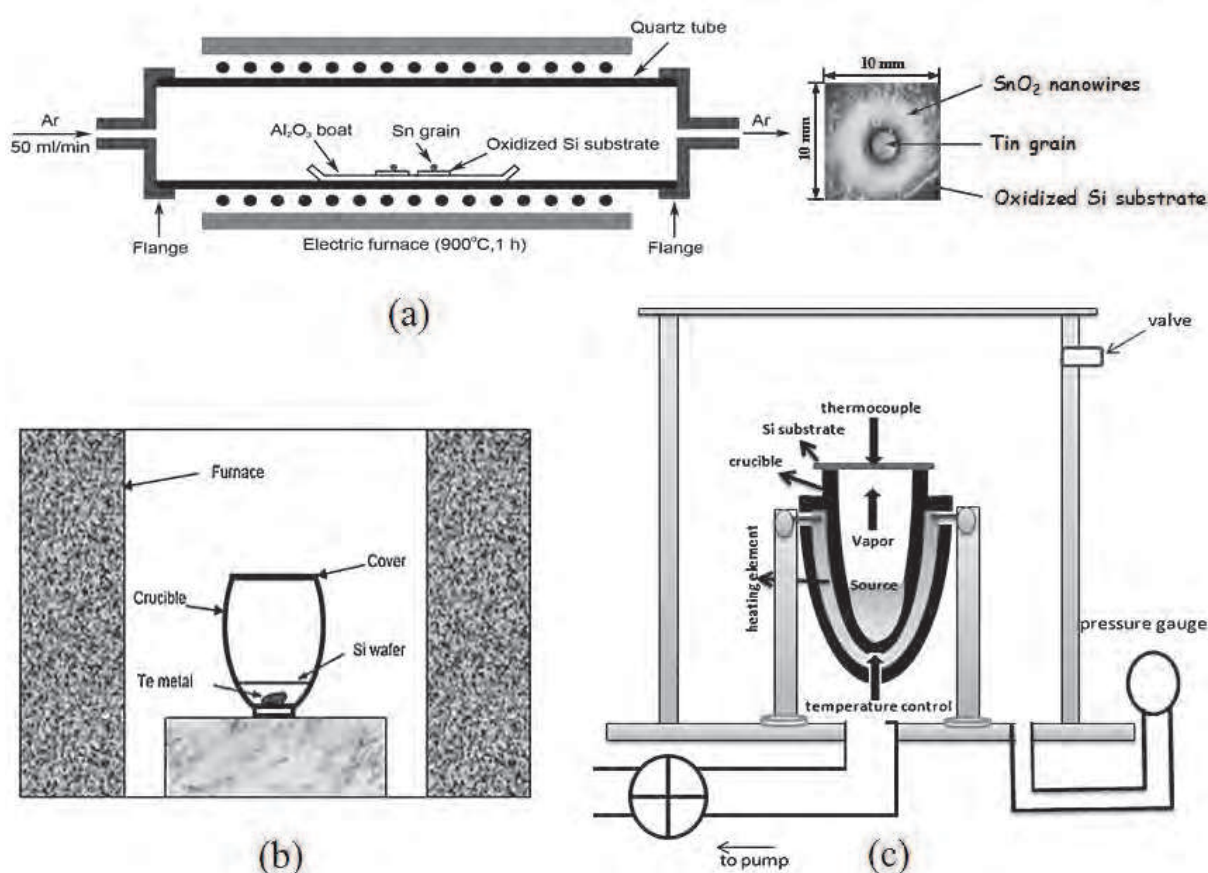

Fig. 1. Formation of oxide semiconductor nanowires. (a) Vapor transport method. (b) Evaporation in ambient air. (c) Modified gas evaporation with a conventional vacuum evaporator.

2.2 Evaporation in ambient air

This method, in which nanowires are formed in an ambient air, is very simple and was applied to the formation of TeO_2 nanowires (Liu et al., 2007; Liu et al., 2008). As shown in Fig.1(b), a desirable amount of tellurium grains at a high purity of 99.999% was placed in an alumina crucible 30mm in height and 20mm in diameter. A piece of oxidized Si substrate was placed about 2mm above the tellurium grains to collect the products. The crucible was covered and heated in a box type furnace at a temperature of 300–500°C for 2 hours. A layer of white product was obtained on the under surface of the substrate.

2.3 Modified gas evaporation

A method, shown in Fig. 1(c), uses a conventional vacuum evaporator. This method, which we call modified gas evaporation method, was applied to the formation of SnO_2 nanowires. The gas evaporation method has been usually used for the formation of metal nanoparticles, which is attained by evaporating metals in vacuum chamber filled with a low pressure (10–1000 Pa) of an inert gas such as helium or argon (Kimoto et al., 1963). It can also be applied to the formation of oxide nanoparticles (Kaito et al., 1977). In the method used here, Sn grains, SnO powder, or SnO_2 powder as a raw material was placed at the bottom of an alumina crucible, and the crucible was covered with an oxidized Si substrate. The crucible was then heated at a high temperature under a low pressure of ambient air. In this configuration, discriminating structures such as nanowires were formed because the substrates on the crucible were also heated at a high temperature.

3. Structure and gas sensing properties of nanowire sensors

3.1 SnO_2 nanowires formed by vapor transport

SnO_2 is the gas sensing material that has been most extensively studied (Windischmann & Mark, 1979; Heiland, 1982; Tamaki et al., 1989). SnO_2 nanowires have also recently been studied vigorously as a gas sensing material (Ramirez et al., 2007; Kumar et al., 2009). In addition to undoped SnO_2 nanowires, we investigated Pd-doped and Pt-doped nanowires, for noble metal doping such as Pd or Pt often improves sensitivity by activating the surface reaction of the gas sensing materials (Yamazoe et al., 1983; Tsang et al., 2001). Because the effect of Pd doping and that of Pt-doping on sensor response were similar to each other, we introduce here only the undoped and Pd-doped nanowire sensors, leaving out Pt-doped nanowire sensors (Shen et al., 2009).

In order to obtain Pd-doped nanowires, 40 µl of ethanol solution of $PdCl_2$ at a concentration of 1×10^{-3} mol/ml or 2.5×10^{-3} mol/ml were dropped on nanowires dispersed on an oxidized Si substrate. The nanowires thus obtained were annealed at 350°C in air for half an hour. The concentration of Pd was estimated to be 0.8 and 2.0 wt%. According to the measurement of X-ray diffraction (XRD) patterns, the SnO_2 nanowires were identified to be tetragonal SnO_2 (JCPDS card No. 41-1445). Figure 2(a) shows a typical scanning electron microscopy (SEM) image of undoped SnO_2 nanowires. The inset shows a high magnification image. SnO_2 nanowires of 30–200 nm in diameter and several tens of micrometers in length are observed. A transmission electron microscopy (TEM) image of an undoped SnO_2 nanowire is shown in Fig. 2(b). A high-resolution TEM (HRTEM) image of this nanowire and its selected area electron diffraction (SAED) pattern represented in Fig. 2(c) indicate that a nanowire is a single crystal. The interplanar spacing of 0.34 nm indicated in Fig. 2(c) corresponds to the (110) plane of a tetragonal SnO_2. The growth direction of SnO_2 nanowire is [301], which is consistent with previous reports (Chen et al., 2003; Wang et al., 2004). The TEM image of a 2 wt% Pd-doped SnO_2 nanowire in Fig. 3(a) shows that dark spots distribute randomly on the surface. An HRTEM image (Fig. 3(b)) shows that they are 3–7nm in diameter. The microbeam diffraction pattern measured for a spot shown in the inset of Fig. 3(b) indicates that the dark spots are PdO particles. According to EDX analysis (Fig. 3(c)), SnO_2 nanowires are surely doped with Pd. No Cl-related signal was observed in the spectrum.
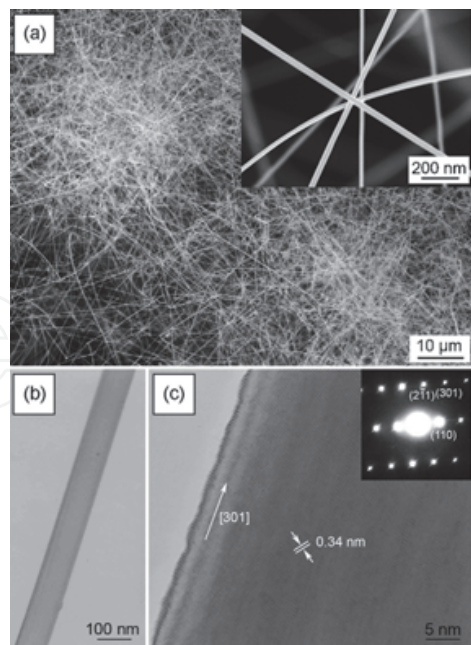
Fig. 2. SEM (a), TEM (b), and HRTEM (c) observation of undoped nanowires.
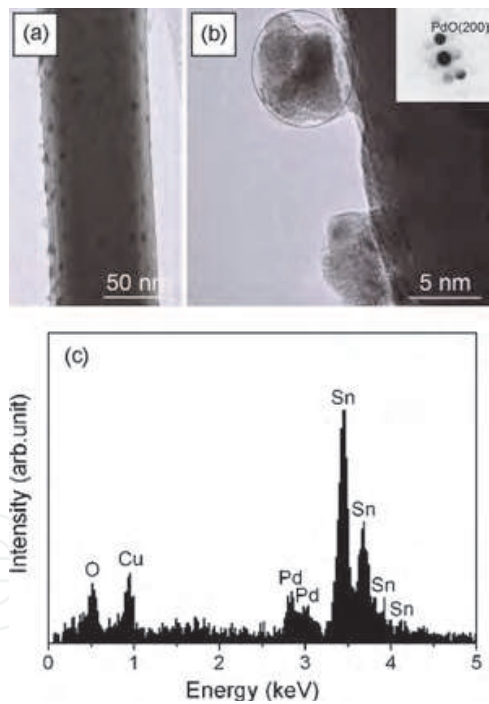

Fig. 3. TEM (a), HRTEM (b), and EDX (c) observation of Pd-doped nanowires.

Sensor devices, illustrated in Fig. 4, were fabricated by dropping nanowire-suspended ethanol on an oxidized Si substrates equipped with a pair of interdigitated Pt electrodes. The gap length of the electrodes was 120 µm. The weight of SnO_2 nanowires dispersed on a sensing element with sizes of 7 mm × 10 mm was 500 µg. The gas sensing properties were measured for the sensors placed in a quartz tube inserted into a tubular electric furnace. Dry synthetic air, mixed with a desired concentration of H_2, flowed at a rate of 200 ml/min.

The changes in the resistance of the sensors made of undoped, 0.8 wt%Pd-doped, and 2 wt%Pd-doped SnO_2 nanowires upon exposure to H_2 at 150°C are shown in Figs. 5(a). The resistance decreases upon exposure to H_2. The decrease in the resistance is expanded as the H_2 concentration increases. The resistance recovers to its initial value after H_2 removal, indicating a good reversibility of these gas sensors. The decrease in the resistance is greatly enhanced by introducing Pd. In Fig. 5(b), the sensitivities defined as Ra/Rg, where Ra and Rg are the resistance before and after exposure to a gas (H_2), respectively, are shown as functions of operating temperature for the three sensors described above. Pd doping improves the sensitivity and lowers the operating temperature at which the sensitivity is maximized.

Now, we compare nanowire sensor with sputtered film sensor. Figure 6 shows the temporal change in the resistance upon exposure to H_2 at a temperature of 100°C. The sensors compared are the one made of nanowires doped with 2 wt% Pd and the one made of porous sputtered film doped with 8 wt% Pd. The operating temperature is 100°C. The latter sensor was made of a Pd-doped porous sputtered film. It showed a high sensitivity to H_2. Although the sensitivity of the Pd-doped nanowire sensor is lower than that of the porous Pd-doped sputtered film, the response time and recovery time of the former are shorter than those of the latter. The short response time and recovery time of the nanowire sensor may be related to the single crystalline character of the nanowires. Because a sputtered film is composed of columnar grains made of fine crystallites, it has narrow voids between columnar grains as well as grain boundaries between the crystallites. When the sputtered film sensor is exposed to H_2, the reconstruction of surface atoms and adsorbed species spreads into the voids and boundaries, being accompanied by atomic diffusion through voids and boundaries. Such a diffusion process may delay the completion of the reconstruction process. On the other hand, the nanowire sensor, which is not accompanied by such a process, may show a quick response and recovery.
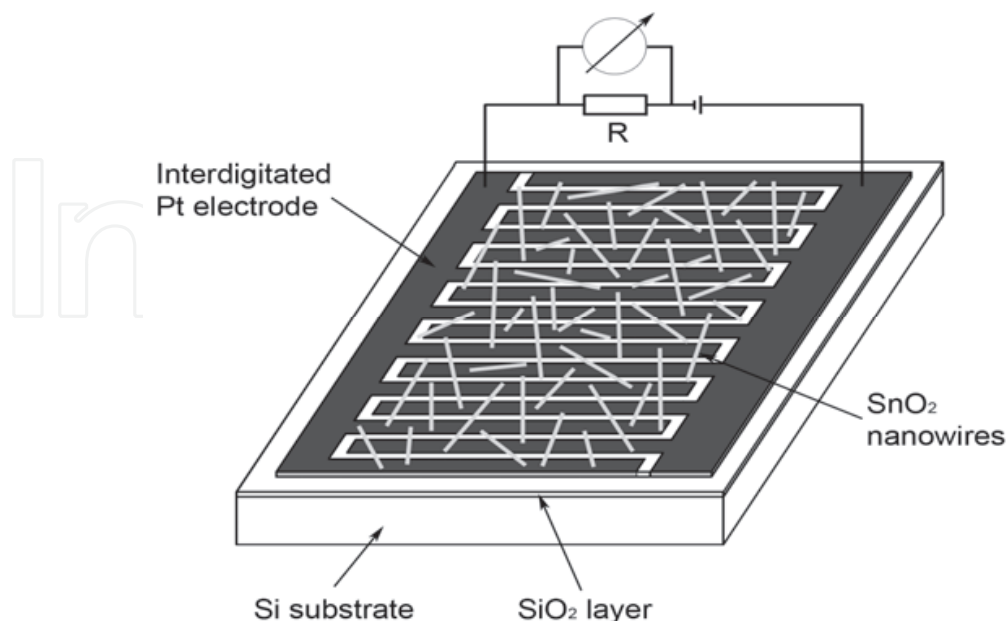

Fig. 4. Schematic diagram of a gas sensor made of nanowires dispersed on a pair of interdigitated electrodes.
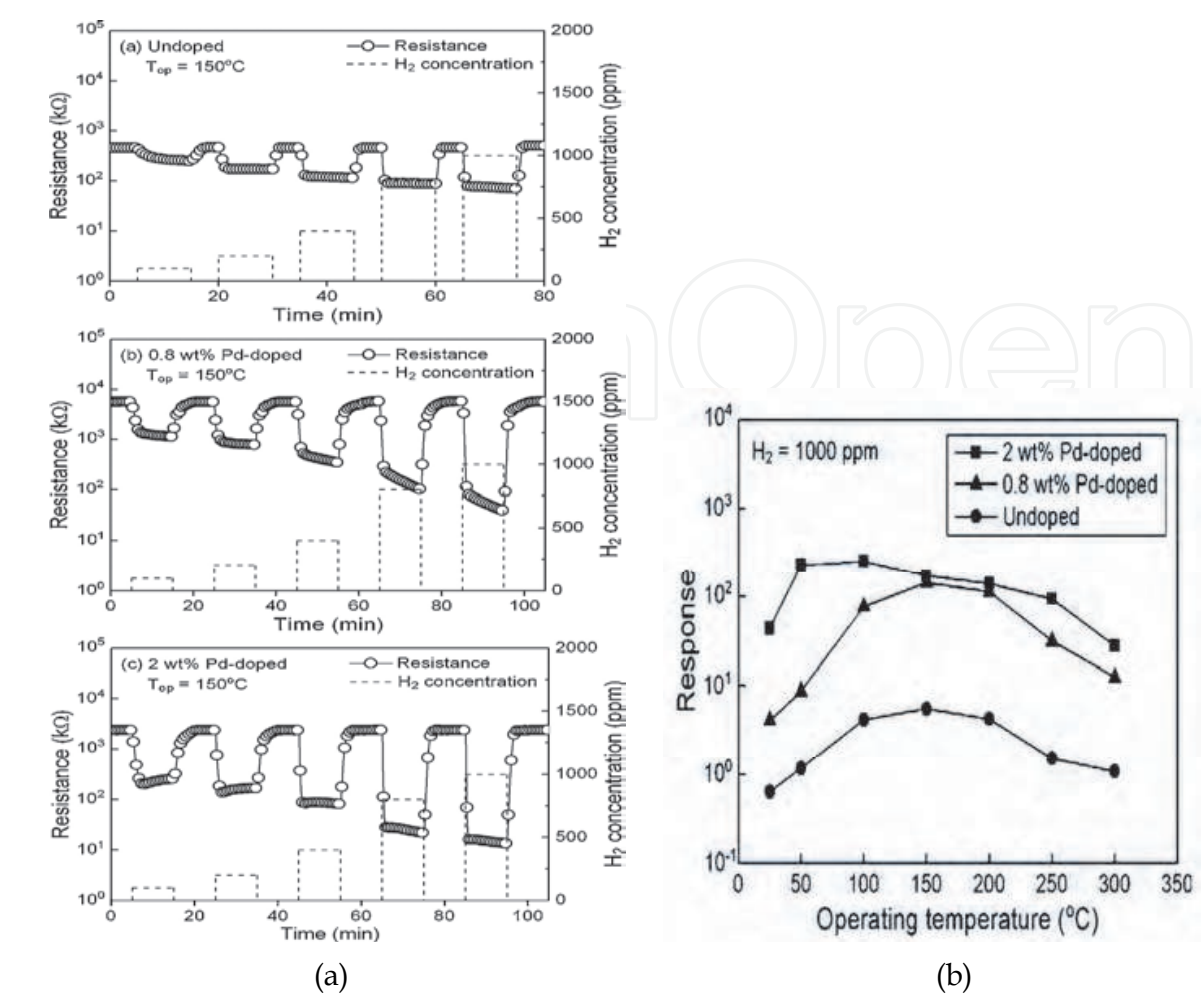
Fig. 5. (a) Changes in the resistance upon exposure to H_2 measured at 150°C. (b) Sensitivity as a function of temperature.
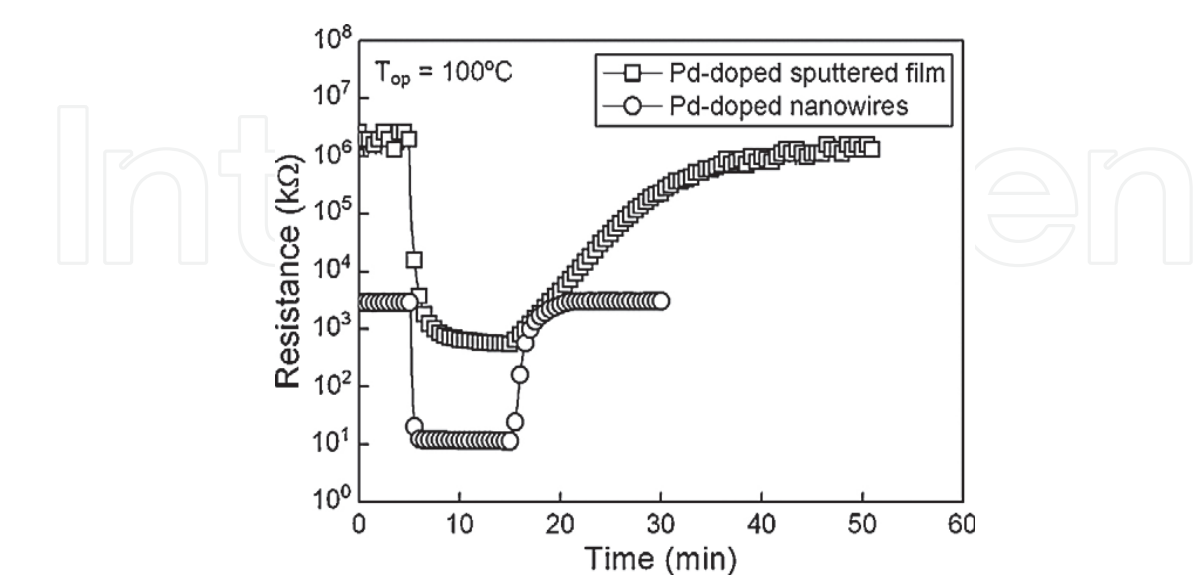

Fig. 6. Changes in the resistance of the 2 wt% Pd-doped nanowire sensor and a porous Pd-doped sputtered film sensor upon exposure to 1000ppm H_2 gas at 100°C .

To clarify the dependence of the response on the operating temperature, the resistances of the undoped and 2 wt% Pd-doped sensors are shown as a function of temperature in Fig. 7, where the values before and after exposure to H_2 are indicated by closed and open symbols, respectively. We see that both the resistance and its temperature dependence are relatively small for the undoped sensor whereas both are large for the 2wt% Pd-doped sensor. In the undoped sensor, oxygen atoms adsorbed on the surface of SnO_2 nanowires in air obtain electrons from the surface region of SnO_2. Thus, a substantial region of each nanowire is depleted of electrons, which results in the high resistance of the sensor. With increasing temperature, the electrons trapped by adsorbed oxygen are thermally excited to the conduction band, causing a decrease in the resistance. When SnO_2 nanowires are exposed to hydrogen, the density of adsorbed oxygen decreases because of the reaction between hydrogen and adsorbed oxygen, which results in a decrease in the resistance. When SnO_2 nanowires are decorated with PdO particles, electrons transfer from SnO_2 to PdO as well as to adsorbed oxygen atoms because the work function of PdO is larger than that of SnO_2 (Jang. et al., 2006; Shimizu et al., 2007). Thus, each nanowire is depleted of electron in its whole region. Therefore, the resistance of the sensor is extremely high in air. When hydrogen is introduced, PdO is reduced to metallic palladium, returning electrons to SnO_2. Hydrogen molecules adsorbed on palladium simultaneously spill over the surface of SnO_2, activating the reaction between hydrogen and the adsorbed oxygen (Yamazoe et al., 1983; Tsang et al., 2001). These phenomena result in an effective shrinkage of the depletion region and lower the resistance of the Pd-doped sensor compared with that of the undoped sensor, leading to a higher response. Because the effect of Pd is active at a relatively low temperature, the sensitivity of Pd-doped sensor is rather high even at room temperature.
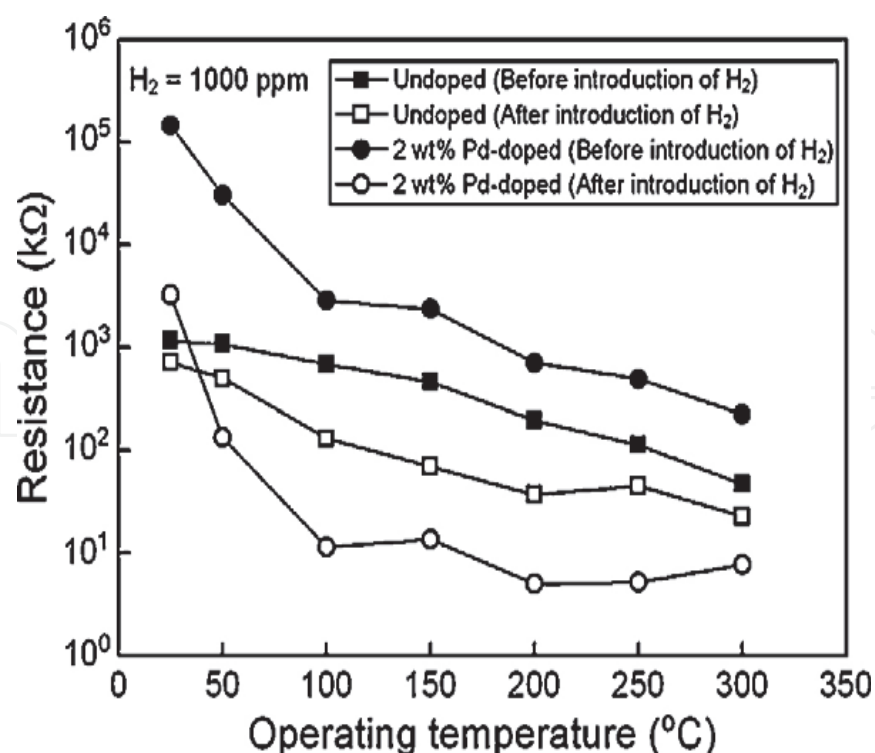

Fig. 7. Temperature dependence of the resistances measured for the undoped and 2 wt% Pd-doped SnO_2 nanowire sensors before and after introduction of H_2.

3.2 WO$_3$ nanowires formed by vapor transport

WO$_3$ has been extensively studied as a material suitable for NO$_2$ sensing (Chung et al., 1999; Jin et al., 2005) since it was shown that it indicated a higher sensitivity to NO$_2$ than to CO, H$_2$, CH$_4$, and i-C$_4$H$_{10}$ (Akiyama et al., 1991). NO$_2$ sensors made of WO$_3$ nanowires have also been studied; the sensors made of nanowires formed by using thermal evaporation (Ponzoni et al., 2006) and solvothermal method (Rout et al., 2006) indicated high sensitivities to NO$_2$ in the range of parts per billion at high temperatures above 200°C. Sensors made of WO$_3$ nanowires formed by using the vapor transport method have been investigated (Cao et al., 2009). They could detect NO$_2$ in the range of parts per billion at 180°C. Sensors made of WO$_3$ nanowires formed by using soft chemistry indicated high sensitivities to NO$_2$ in the range of parts per billion at 150°C (Polleux et al., 2006).

In our study, WO$_3$ nanowires were formed by the vapor transport method using WO$_3$ powder as a raw material. An alumina boat loaded with WO$_3$ powder (100 mg, 99.9% purity) was placed at the center of a quartz tube. A substrate on another alumina boat was placed 16, 17, or 17.5 cm away from the WO$_3$ powder. After the quartz tube was evacuated from the end of the quartz tube at the side of substrate to a pressure of approximately 30 Pa, Ar gas was introduced at a flow rate of 900 ml/min into the quartz tube, which resulted in a pressure of 270 Pa. The temperature of the furnace or the temperature of WO$_3$ powder was then increased to 1050, 1100, or 1150°C. After maintaining the furnace at these temperatures for 2 hours, the furnace was cooled naturally to room temperature. It should be noted that the substrate temperature was lower than the furnace temperature. Table 1 shows the temperatures of the substrates placed 16, 17, or 17.5 cm away from the WO$_3$ powder at various furnace temperatures. Our attempt to deposit a product on an oxidized Si substrate failed. Thus, an oxidized Si substrate coated with Au film 5 nm thick was used to deposit the product.

SEM images of the products are shown in Fig. 8. The morphology of the products depends on the furnace temperature and substrate position. We refer to all of the products as nanowires for convenience, although the products deposited at 1050°C are better described as nanostrips. It was difficult to peel the nanowires deposited at 1050°C from the substrate. The nanowires formed at 1100 and 1150°C were in a powdered form, i.e., they were easily peeled from the substrates. The diameter of the nanowires decreased as the distance of the substrate from the WO$_3$ powder as a raw material increased. Thin nanowires were formed at a furnace temperature of 1100°C. In this condition, the thinnest nanowires with a diameter of 50 nm were formed 17.5 cm away from the WO$_3$ powder. According to XRD, all products were hexagonal WO$_3$ listed in JCPDS card No. 85-2460. Note that this structure is different from those reported for the nanowires formed using the vapor transport method by other research groups. WO$_3$ nanowires with a monoclinic structure (Cao et al., 2009) and W$_{18}$O$_{49}$ nanowires with a monoclinic structure (Hong et al., 2006) have been reported. The hexagonal structure that we obtained agrees with that of the nanowires formed by a solvothermal method (Choi et al., 2005). According to TEM observation, a nanowire was a single crystal and its growth direction was [001].

Sensors were fabricated by poring a few drops of nanowire-suspended ethanol onto oxidized Si substrates equipped with a pair of Pt interdigitated electrodes with a gap length of 35 μm and an element area of 9 × 10 mm². The weight of the dispersed nanowires was 200 μg. The measurement of the sensing properties was performed in the same manner as that for the SnO$_2$ nanowire sensors.

Furnace temperature (°C)	Substrate temperature (°C)		
	Position of 16 cm	Position of 17 cm	Position of 17.5 cm
1050	490	300	230
1100	520	330	250
1150	550	350	270

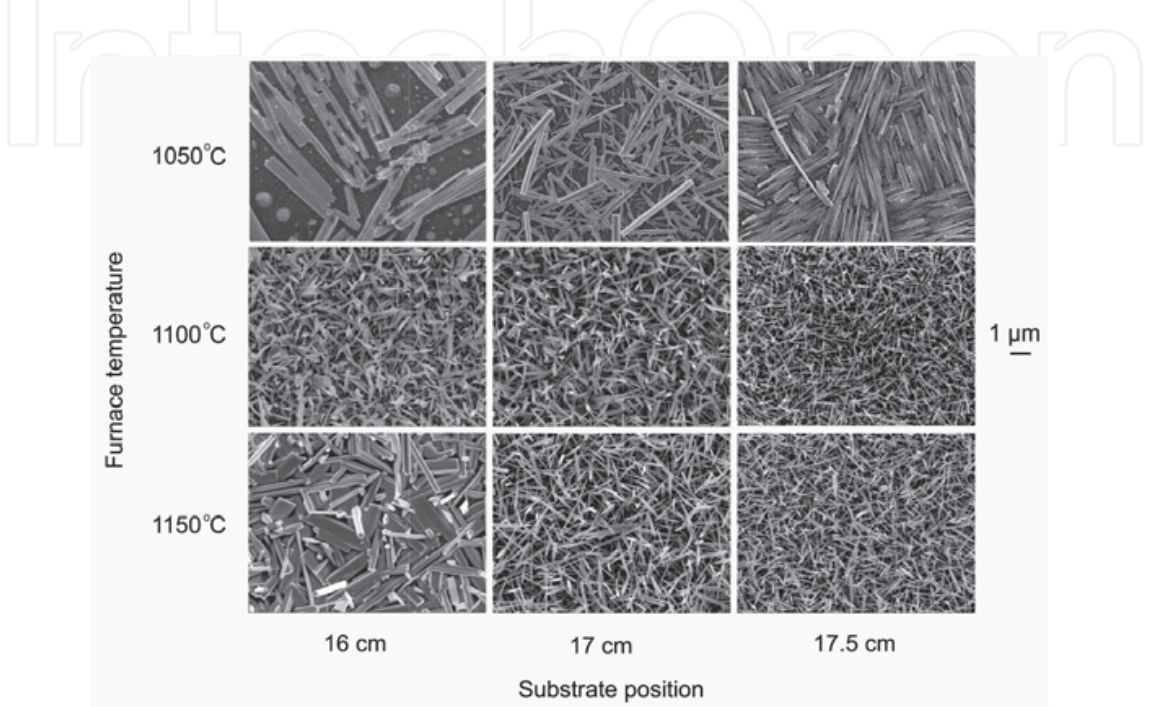Table 1. Substrate temperature at different positions for different furnace temperatures.

Fig. 8. SEM images of the products deposited at different positions and different furnace temperatures.

The temporal responses to NO_2 at 3 ppm measured for a sensor made of nanowires as thin as 50 nm, deposited on a substrate 17.5 cm away from the WO_3 powder at a furnace temperature of 1100°C, are represented in Fig. 9(a). The results are shown for the operating temperatures of 50, 150, and 250°C. The resistance decreases as the temperature increases. When the sensor is exposed to NO_2, the resistance quickly increases. After the removal of NO_2, the resistance recovers to the initial value in approximately 10 min at a high temperature of 250°C. However, it recovers more slowly at a lower temperature. Figure 9(b) shows the temperature dependence of the sensitivity defined as (Rg-Ra)/Ra. The results for the sensors made of the nanowires deposited at different positions at 1100°C (upper figure) and those for the sensors made of the nanowires deposited on a substrate at 17.5 cm at different temperatures(lower figure) are represented. All sensors, made of nanowires with different diameters, have a peak operating temperature at which their sensitivities are maximized. While NO_2 sensing due to electron transfer from oxide to adsorbed NO_2, which forms NO_2^- (Ruhland et al., 1998), is thermally activated with increasing temperature, the decrease in sensitivity at temperatures above the peak temperature suggests the change in surface reaction. Recent spectroscopic studies (Sergent et al., 2007; Lebranc et al., 2000) demonstrated that at higher temperatures adsorbed species for NO_2 gas is NO_3^- rather than NO_2^-, which suggests that NO_2 gas does not react directly with oxide but react with a high

density of adsorbed O⁻, forming NO_3^- (Francioso et al., 2006) and not contributing to increase in the resistance. The peak temperature decreases as the diameter of the nanowires decreases. The highest sensitivity obtained in this study was 37, which was observed at 100°C for the thinnest nanowires with a diameter of 50 nm.

The sensitivities at 100°C are summarized as a function of the average diameter of the nanowires in Fig. 10. The relationship between the sensitivity and diameter is expressed by a unique curve, indicating that the sensitivity increases with decreasing diameter.

(a)   (b)
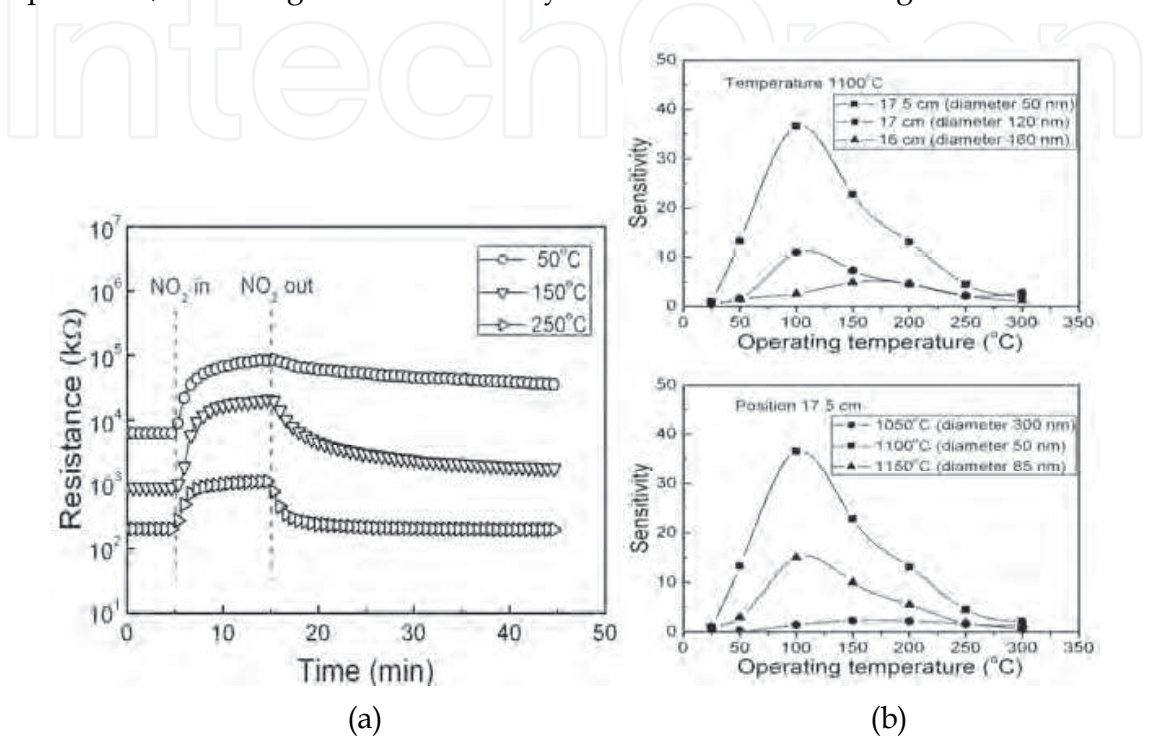
Fig. 9. (a) Change in resistance of WO_3 nanowire sensor upon exposure to NO_2 at 3 ppm at different operating temperatures. (b) Operating temperature dependence of sensitivity to NO_2 measured for the nanowires wih different diameters.
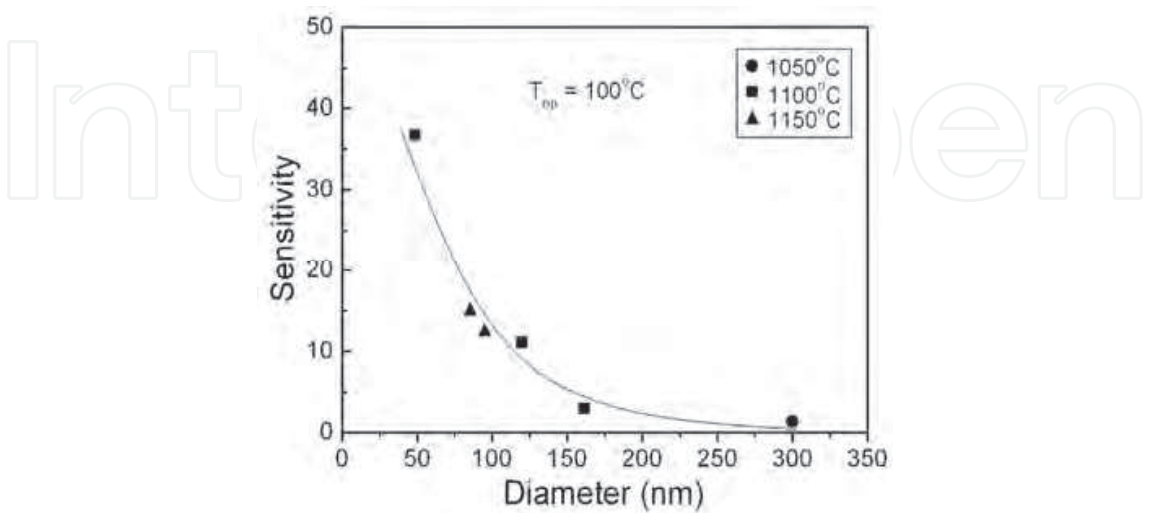

Fig. 10. Sensitivity at 100°C as a function of the diameter of nanowires. The sensitivities of the sensors made of nanowires deposited at different furnace temperatures are plotted.

3.3 Ga$_2$O$_3$ nanowires formed by vapor transport

Ga$_2$O$_3$ thin films have been studied as a gas sensor operating at a high temperature because of their stability at a high temperature. For example, they have been studied as oxygen sensors operating at 600–1000°C (Babana et al, 2005; Schwebel et al., 2000). They have also been studied as sensors for detecting reducing gases such as H$_2$, CO, CH$_4$ (Fleisher et al., 1992; Schwebel et al., 1998). Ga$_2$O$_3$ nanowires have also been studied as gas sensing materials (Liu et al., 2008; Mazeina et al., 2010).

In our study, a gallium grain (99.999%, 0.5 g) was placed on an alumina substrate in an alumina boat (Liu et al., 2008). The grain was then heated in a tube furnace at 900°C for 1 hour in an Ar flow of 100 ml/min at ambient pressure. After cooling to room temperature, a layer of white product was obtained on the alumina substrate around the gallium grain.

An SEM image in Fig. 11(a) shows that the obtained nanowires are about 50–150 nm in diameter and tens of micrometers in length. The XRD pattern in Fig. 11(b) agrees with the pattern of monoclinic β-Ga$_2$O$_3$ (JCPDS card No. 43-1012). A TEM image of the nanowires with a diffraction pattern, shown in Fig. 11(c), confirms the formation of single-crystal monoclinic Ga$_2$O$_3$. In our study, the Ga$_2$O$_3$ nanowires were formed in an Ar flow, which provided a lean oxygen environment. Therefore, the Ga$_2$O$_3$ nanowires obtained contain a high concentration of oxygen vacancies. This is confirmed by photoluminescence (PL). As shown in Fig. 11(d), the PL spectrum of the nanowires shows a broad strong PL peak at about 440 nm. According to literature (Binet & Gourier, 1998), the broad blue luminescence at 400–500 nm is ascribed to the electron transition mediated by oxygen vacancies in the band gap. These oxygen vacancies contribute to the n-type electrical conduction of the Ga$_2$O$_3$ nanowires.
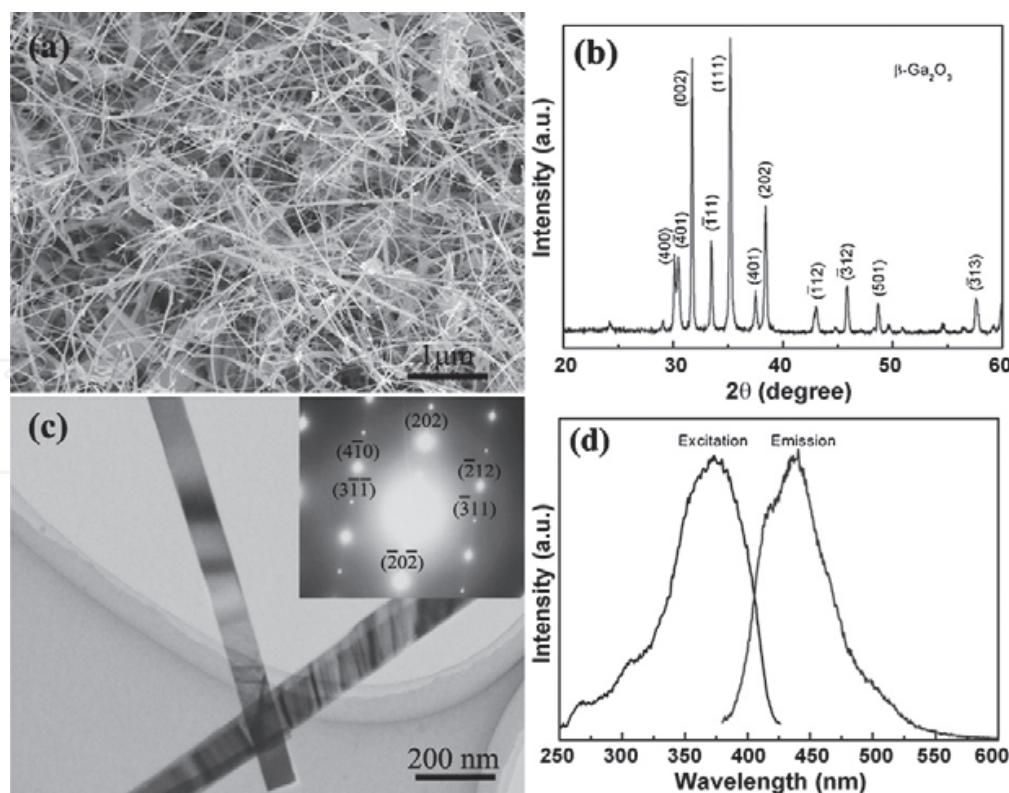

Fig. 11. (a) SEM image, (b) XRD pattern, (c) TEM image with diffraction pattern, and (d) photoluminescence spectrum of Ga$_2$O$_3$ nanowires.

Gas sensors were fabricated by dispersing nanowires on an oxidized Si substrate equipped with Pt electrodes with a gap length of 40 μm. Their gas sensing property was evaluated for O_2 in nitrogen and CO in dry synthetic air. The sensors showed obvious responses to O_2 and CO at temperatures much lower than that reported for Ga_2O_3 film sensors. Reversible changes in resistance upon introduction and removal of O_2 at 300°C is shown in Fig.12.

Figure 13 shows the sensitivity, defined by (Rg-Ra)/Ra for O_2 at 1% and (Ra-Rg)/Rg for CO at 200 ppm, measured at 100–500°C. It shows that the temperature dependence indicates a peak for both O_2 and CO. The highest sensitivity to 1% O_2 is 4.8 at 300°C, while the value to CO is 4.0 at 200°C. It is important to note that the operating temperature of our Ga_2O_3 nanowire sensor is much lower than 600–1000°C reported for Ga_2O_3 film sensors. This fact expands the application of Ga_2O_3 sensors to low operating temperatures.
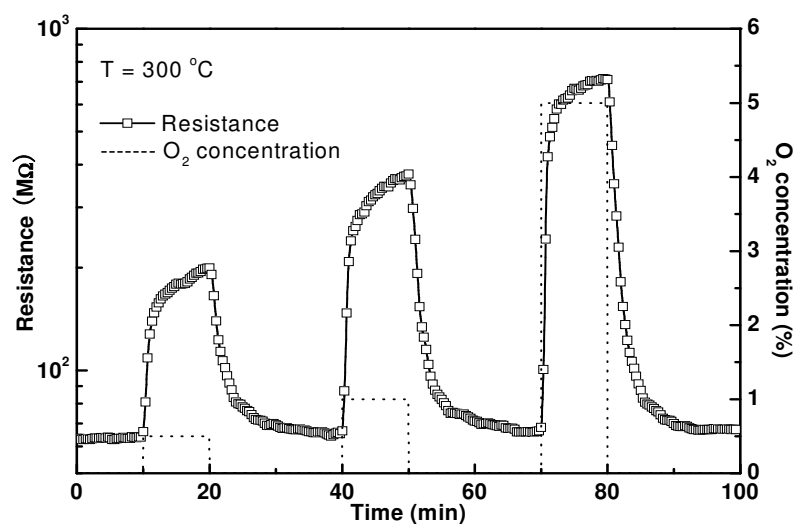

Fig. 12. Temporal changen in the resistance of a Ga_2O_3 nanowire sensor upon exposure to O_2 at 300°C.
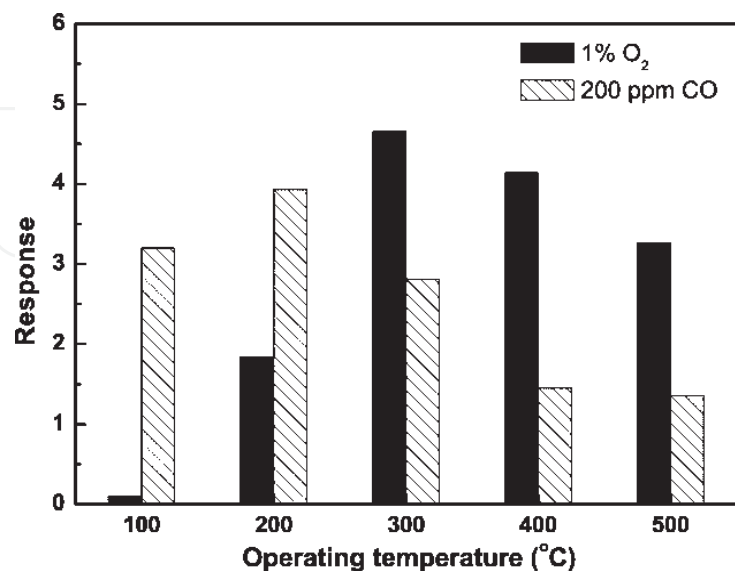

Fig. 13. Temperature dependence of the sensitivity of the Ga_2O_3 nanowire sensor to O_2 and CO gases.

3.4 TeO$_2$ nanowires formed by evaporation in ambient air

There have been no reports on the formation of TeO$_2$ nanowires. Figure 14 shows the typical SEM image of the nanowires that we formed by thermal evaporation of Te grains in ambient air (Liu et al., 2007; Liu et al., 2008). The nanowires are several tens of micrometers in length and 30–200 nm in diameter. According to XRD, the nanowires obtained were a tetragonal TeO$_2$ (JCPDS No. 11-0693). Figure 15(a) shows a typical TEM image of the TeO$_2$ nanowires. The HRTEM image and diffraction pattern in Figs. 15(b) and 15(c) show that a nanowire is a single crystal. The lattice spacings 0.47 and 0.29 nm observed in the HRTEM image correspond to those of (010) and (102) planes of a tetragonal TeO$_2$, respectively.

It was found that heating temperature and time were two crucial parameters in the determination of the morphology of the products. According to XRD, all products obtained were tetragonal TeO$_2$. Micro-sized wires were obtained at a temperature higher than 450°C, while only a small amount of particles were obtained at 300°C. The heating temperature of 400°C was optimal for the growth of TeO$_2$ nanowires. However, it is noticeable that a thin layer of TeO$_2$ particles was formed before the growth of TeO$_2$ wires in all cases. These particles may have played an important role in the growth of TeO$_2$ nanowires.

Gas sensors were fabricated using electrodes with a gap length of 40 µm. Test gases were added to a dry synthetic air with a total gas flow rate fixed at 200 ml/min. The temperature of the sensors was kept at room temperature (26°C). Figures 16(a)–16(c) show the change in the resistance upon introduction and exhaust of NO$_2$, NH$_3$, and H$_2$S at different concentrations. The resistance decreases quickly upon introduction of NO$_2$. The change in resistance can reach 90% of its final change about 2 min after the introduction of NO$_2$. The response to NH$_3$ is relatively slow. The resistance increases even 10 min after exposure to NH$_3$. It does not return to the initial value even 30 min after exhaust of NH$_3$, implying a slow surface reaction on the TeO$_2$ surface. The resistance changes reversibly upon introduction and exhaust of H$_2$S. However, the change in the resistance upon exposure to H$_2$S is much reduced at a concentration lower than 50 ppm, and the sensitivity is negligible at a concentration of 10 ppm. Note that the resistance increases upon exposure to oxidizing NO$_2$ while it decreases upon exposure to reducing NH$_3$ and H$_2$S. This implies that the TeO$_2$ nanowires are a p-type semiconductor.
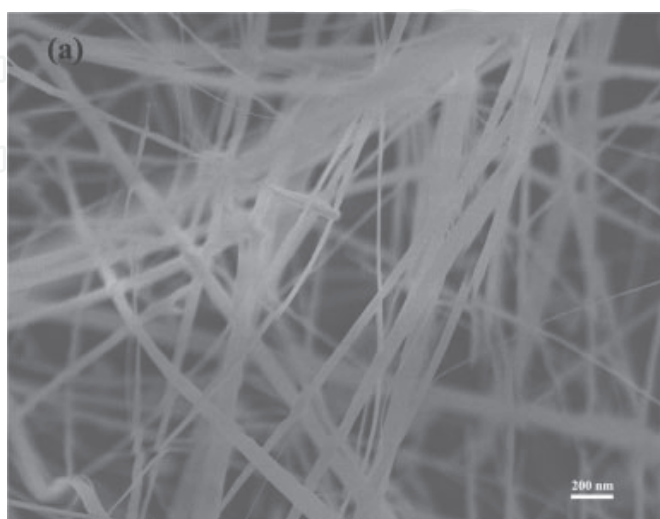

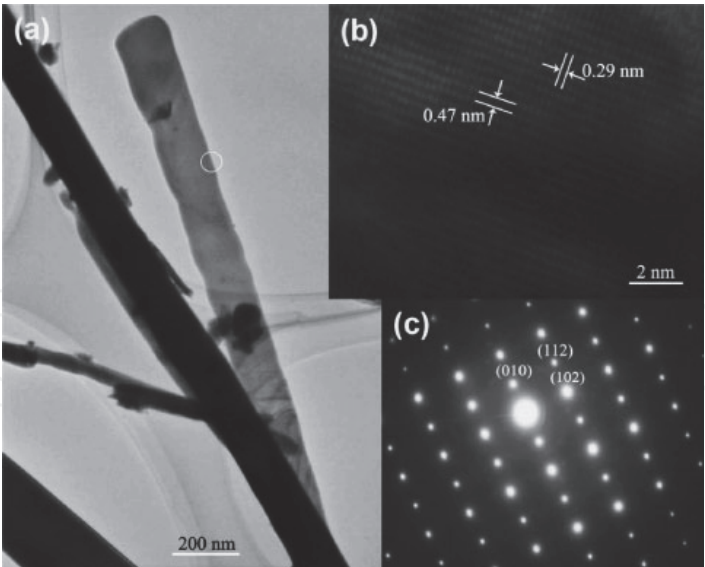Fig. 14. SEM image of TeO$_2$ nanowire.

Fig. 15. TEM image of TeO$_2$ nanowires (a), HRTEM image of a TeO$_2$ nanowire (b), and its diffraction pattern (c).
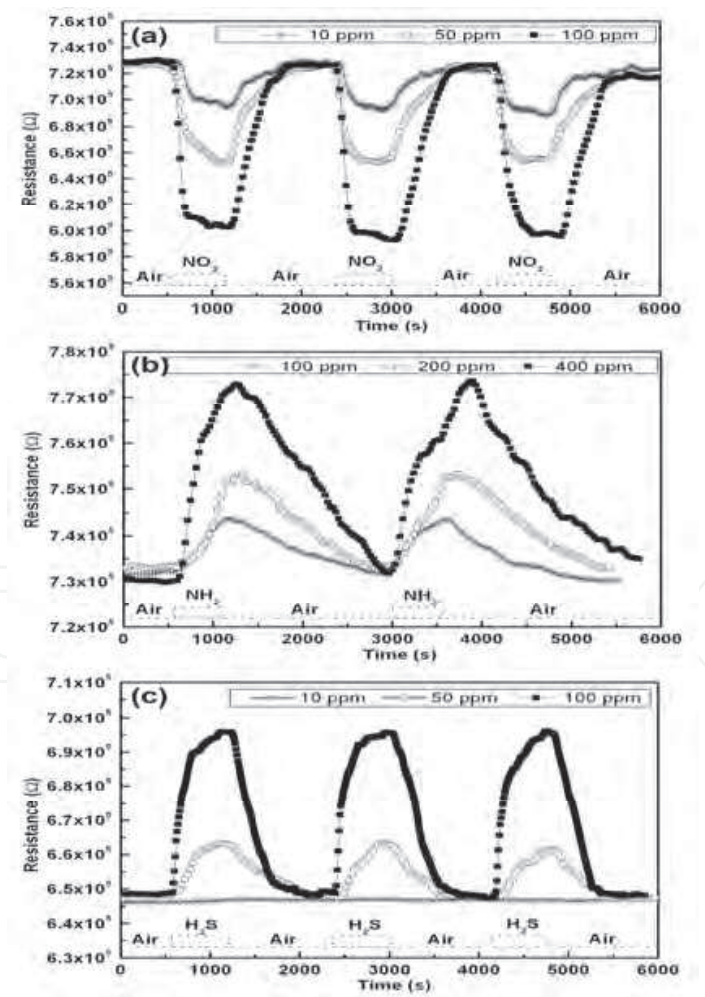

Fig. 16. Change in resistance upon exposure to NO$_2$ (a), NH$_3$ (b), and H$_2$S (c) at different concentrations.

The observation of n-type conduction of TeO_2 at high temperatures above 400°C or low oxygen partial pressure was reported, and it was explained in terms of oxygen vacancies (Jain & Nowick, 1981). However, p-type TeO_2 has also been reported. That is, p-type character has been observed for a single crystal (Hartmann & Kovacs, 1982), thin film (Jain & Garg, 1979), and polycrystal (Doi et al., 1975) by the measurement of Seebeck coefficient or photoconductivity at normal condition. The p-type conduction was ascribed to interstitial oxygen atoms (Doi et al., 1975), which trap electrons, generating holes as majority carriers.

3.5 SnO$_2$ nanowires formed by modified gas evaporation

A crucible containing Sn grains, SnO powder, or SnO_2 powder, each with a purity higher than 99.99%, were heated at 900°C for 90 min under a low pressure of ambient air. The pressures of the air during deposition were 140, 86, and 86 Pa for Sn grains, SnO powder, and SnO_2 powder, respectively.

SEM images in Fig. 17 show that the morphology of the product depends on the raw materials. Microwires (MWs), formed using Sn grains, are about 2 μm in diameter and 20 μm in length. They have rough surface and rectangular cross-section. Nanowires (NWs), formed using SnO powder, are 20 μm in average length and have smooth surface. Their circular cross-sections are 50-100nm in diameter. The rice-shaped nanoparticles (NPs), formed using SnO_2 powder, are about 100 nm in average diameter. XRD patterns showed that all of these materials were SnO_2 with a rutile structure (JCPDS card No.41-1445).

The changes in the resistances of the sensors made of SnO_2 microwires, nanowires, and nanoparticles upon exposure to 2ppm NO_2 at 200°C are shown in Fig. 18(a). The resistances increase upon exposure to NO_2 and recover to their initial values after exhaust of NO_2, indicating a good reversibility. The temperature dependencies of the sensitivities Rg/Ra of these sensors are shown in Fig. 18(b). The sensitivity of nanoparticle sensor is relatively low. The highest sensitivity 5.5 of this sensor was observed at 200°C. The sensitivity of the microwire sensor is slightly higher than that of nanoparticle sensor despite the smaller surface-to-volume ratio of microwires than nanoparticles. The sensitivity of the nanowire sensor is much higher than that of the microwire sensor. The peak temperatures of the sensitivity observed for the microwire and nanowire sensors, namely 100 and 150°C, are lower than 200°C observed for the nanoparticle sensor. The change in the diameter of nanostructure leads to a change in both the sensitivity and peak temperature (Korotcenkov, 2002). The highest sensitivity obtained was 88 at 150°C measured for the nanowire sensor. Thus, we can believe that a sensor made of thin nanowires is suitable for monitoring a low concentration of NO_2.
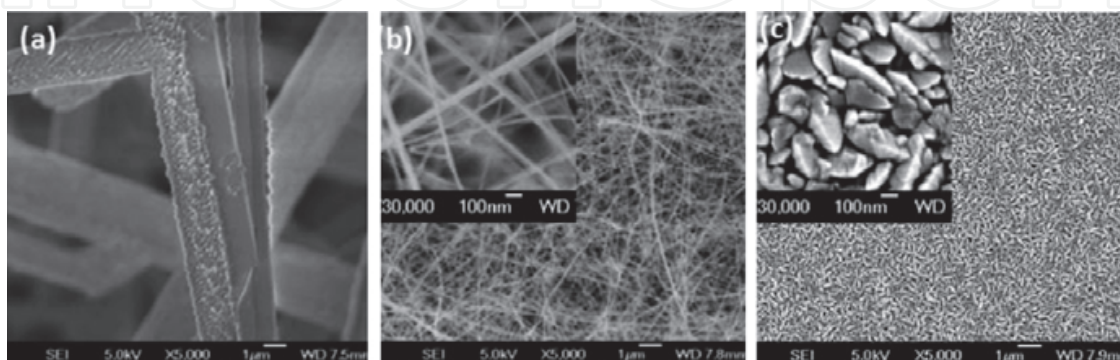

Fig. 17. SEM images of microwires, nanowires, and rice-shaped nanoparticles.

The response and recovery times, defined as the time necessary for the change in resistance upon exposure and exhaust of NO_2 to reach 90% of the whole change, are shown as functions of temperature in Fig. 19. The response and recovery times of microwires and nanowires are shorter than those of nanoparticles. The behavior of the sensitivity as well as response and recovery time shown in Figs. 18 and 19 suggests that the surface reaction depends on temperature. The electron transfer from SnO_2 to adsorbed NO_2, which forms NO_2^-, occurs at relatively low temperatures of 100 and 150°C in microwires and naowires, respectively. This results in the high sensitivities of the microwire sensor and nanowier sensor at these temperatures. At higher temperatures the sensitivity is lowered similarly to WO_3 sensors.

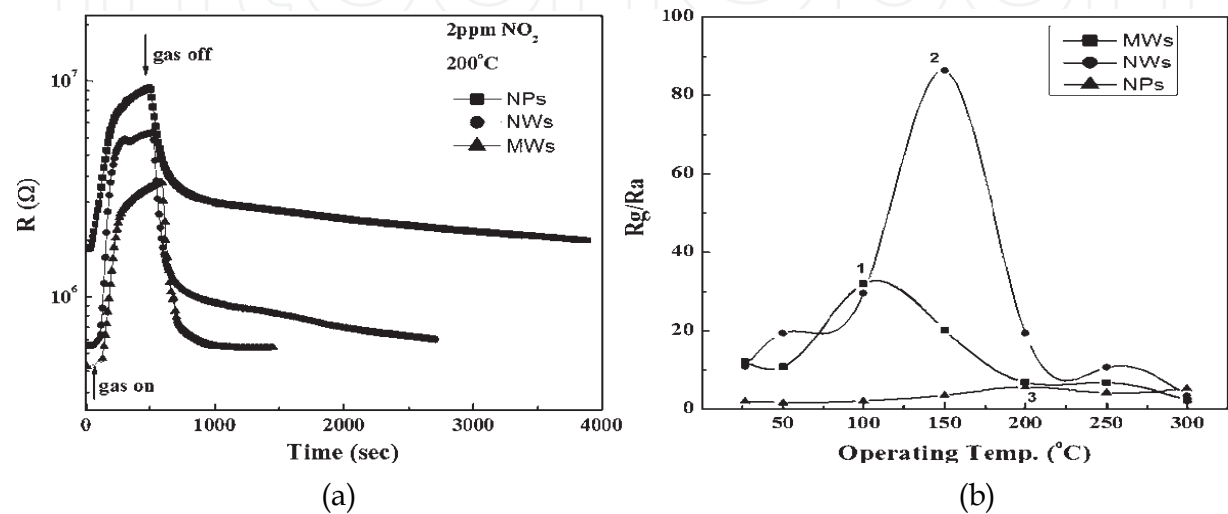(a)   (b)

Fig. 18. (a) Change in the resistances of the sensors made of microwires, nanowires, and rice-shaped nanoparticles upon exposure to 2 ppm NO_2 at 200°C. (b) Sensitivities of the sensors to 2ppm NO_2 as functions of temperature.
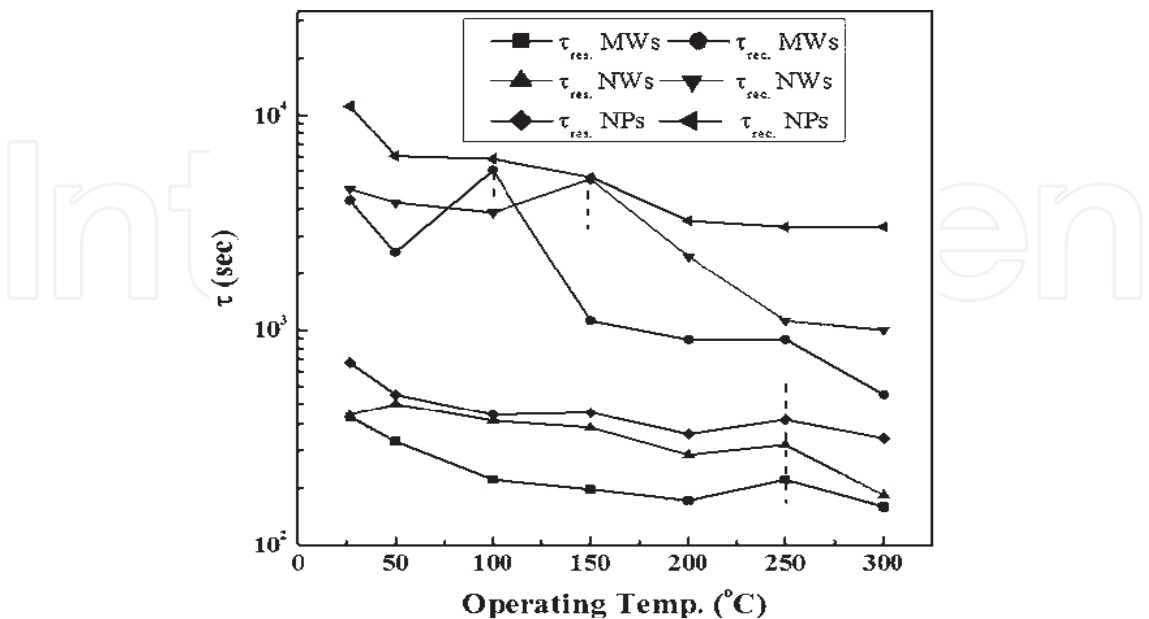

Fig. 19. Recovery and response time of SnO_2 nanowire sensors exposed to 2 ppm NO_2 at a function of temperatures.

Now, we consider the effect of grain size, namely the effect of the diameter of particles or the length of wires. Spherical or wire grains arrayed linearly in the gap between a pair of electrodes are illustrated in Fig. 20, where the grains are assumed to be depleted of electrons only at the surface region of the thickness of L_D. The number of grains in the gap is much smaller in the microwire and nanowire sensors than in the nanoparticle sensor. Therefore, in the microwire and nanowire sensors, the contribution to the sensor resistance of the bulk and the interface between metal electrode and oxide is large while the contribution of grain boundaries is small. As shown in Fig. 20, if the diameter of the grains is small, the highly conductive bulk region is narrow. Thus, the conductance of the bulk region is more affected by its own shrinkage upon exposure to NO_2, leading to nanowires more sensitive to NO_2 than microwires. Although the surface-to-volume ratio of microwires is smaller than that of nanoparticles, the sensitivity of the microwire sensor is larger than that of the nanoparticle sensor. In the sensor of microwires or nanowires, the influence of the resistance of metal-oxide interface on the sensitivity may be larger than that of the resistance of grain boundaries. This seems to lead to the higher sensitivities observed for microwires and nanowires.
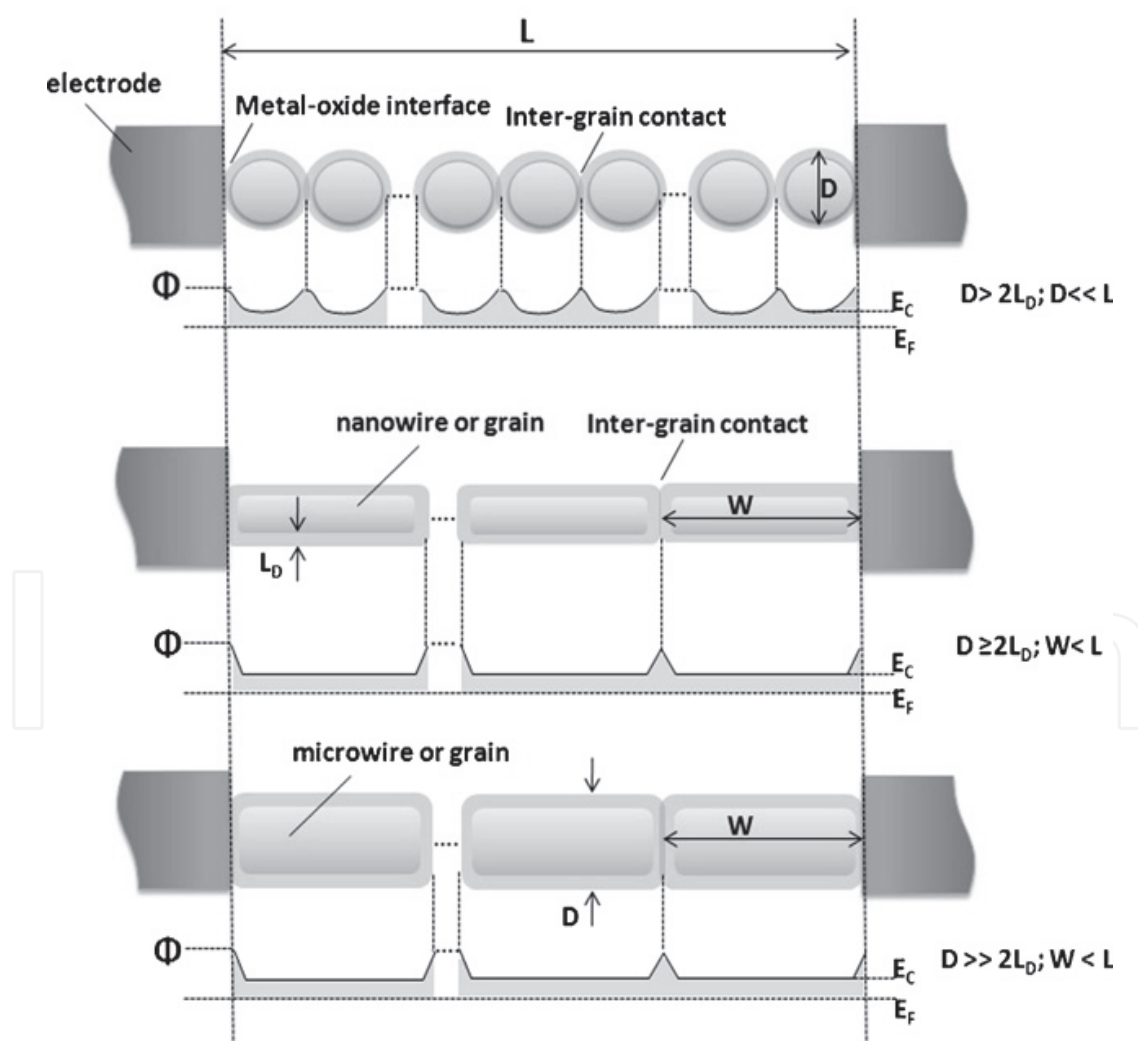

Fig. 20. Model for the distributions of SnO_2 grains. The length and diameter of SnO_2 grains affect the density of grain boundaries and potential distribution.

3.6 Effect of gap length for SnO$_2$ nanowires

If the interface between the metal electrode and oxide is intrinsically important in the determination of the sensitivity of nanowire sensors, as described in the previous section, the sensitivity must be affected by the gap length of a pair of electrodes. Thus, the influence of the gap length was investigated using nanowires formed by heating an Sn grain in a crucible at 800°C at a pressure of 40 Pa of ambient air. The fabrication of a pair electrode, made of an Au sputtered film, is illustrated in Fig. 21. Au-film strip with a width of 2 mm, equipped with a gap formed using field ion beam technology (FIB), is shown at the bottom. Four sensors thus fabricated had a gap length of 1, 5, 10, and 30 μm, respectively.

An SEM image represented in Fig. 22(a) shows that the nanowires obtained are straight with rather uniform length (~5 μm) and diameter (~100 nm). An example of the SEM image of a gap formed by FIB is shown in Fig. 22(b).
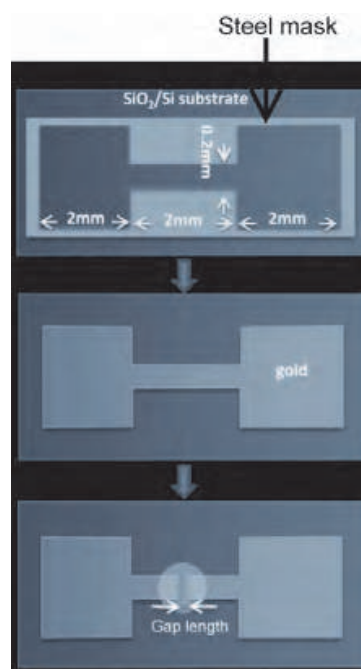

Fig. 21. Fabrication of a pair of gold electrodes. After an Au-film pattern was formed using a steel mask, a short gap was formed using FIB.
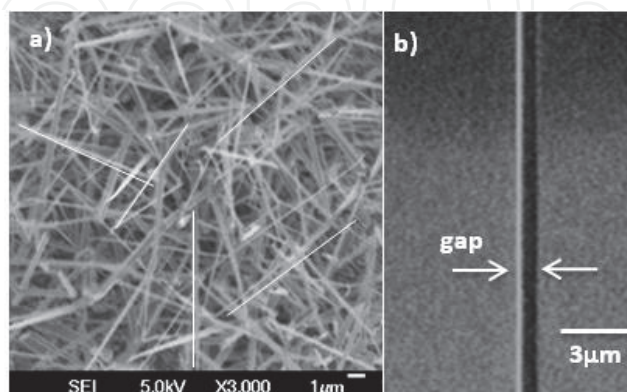

Fig. 22. (a) SEM images of SnO$_2$ nanowires. (b) A micro-gap with a length of 1μm formed by using the method illustrated in Fig. 21.

The change in resistance upon exposure to NO_2 at different concentrations was measured for the four sensors with various gap lengths. The results at 250°C are shown in Fig. 23. The resistance increases upon exposure to NO_2 and decreases upon exhaust of NO_2. The response and recovery speeds increase with decreasing gap length. We notice that the resistance of the sensors with longer gaps does not return to the initial value precisely and that the signal of these sensors is noisy for a higher concentration of NO_2.

Figure 24 shows the sensitivity, Rg/Ra, to NO_2 at 2 ppm as a function of the gap length. The results at various operating temperatures are shown. The sensitivity of the sensor with a gap length of 1 μm, which is shorter than the length of the nanowires, is highest at every temperature. Temperature dependencies of the sensitivity are shown in the inset of this figure. Similarly to the sensors made of WO_3 nanowires, the temperature dependence shows a peak. As the temperature increases, the sensitivities of all sensors increase drastically at a temperature up to 100°C and then decrease at a temperature above 100°C. Thus, the sensitivity at 100°C measured for the sensor with the shortest gap length of 1 μm is as high as 600.

Although the role of the metal-oxide interface is still not clear, it may be due to some kind of chemical sensitization. The so called chemical sensitization in oxide semiconductor gas sensor is mediated by a "spillover effect", and it was experimentally studied for hydrogen and oxygen (Yamazoe et al., 1983; Boudart & Mol, 1999; Bowker et al., 2000; Kolmakov et al., 2005). It is probable that an Au electrode can also act as a catalyst mediating some chemical sensitization. References (Tamaki et al., 2005; Tamaki et al., 2008) discussing NO_2 sensors made of WO_3 nanoparticles equipped with Au nano-gap electrodes suggested that NO_2 gas might be adsorbed in a high density at the interface due to catalytic effect of Au. It was also suggested that the adsorption of NO_2 on an Au electrode might increase its work function. These reactions cause a higher Schottky barrier upon exposure of the sensor to NO_2 gas, leading to a higher resistance or the higher sensitivity, as observed in the sensitivity of the sensor with a short gap length of 1μm.
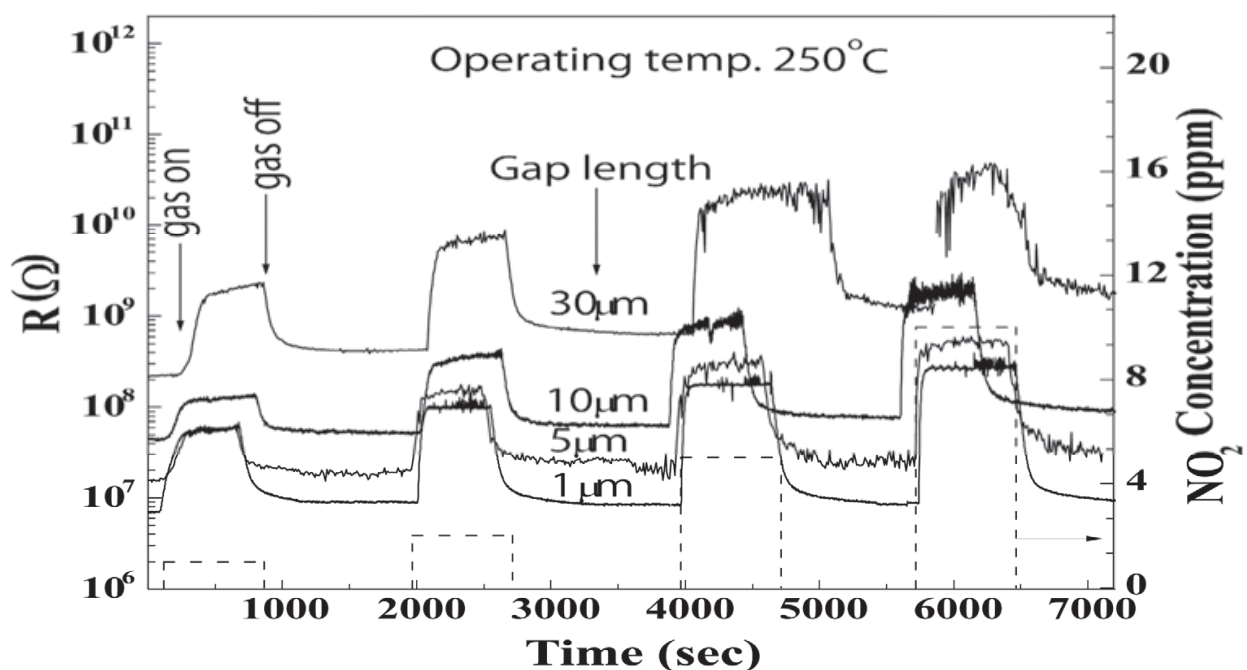

Fig. 23. Change in the resistances of SnO_2 sensors with different gap lengths upon exposure to different concentrations of NO_2 gas at 250°C.
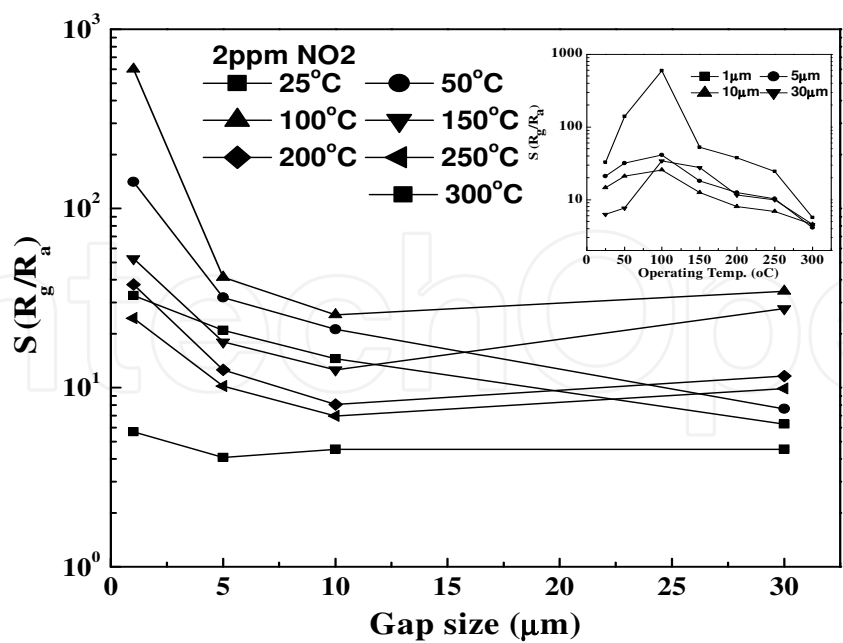
Fig. 24. Sensitivity to NO$_2$ at 2 ppm as a function of the gap length. The results at various temperatures are shown. The inset shows the same data but versus the operating temperature.

4. Conclusions

These ten years, various kinds of oxide semiconductor nanowires have been studied as gas sensing materials because of their large surface-to-volume ratio leading to a high sensitivity and also because of their discriminating morphology which may lead to unexpectedly excellent properties. We attempted to develop various types of thermal evaporation method for making various kinds of oxide nanowires and also attempted to clarify the feature of the gas sensing properties of nanowire sensors. Conventional vapour transport method was used for the formation of SnO$_2$, WO$_3$, and Ga$_2$O$_3$ nanowires. A very simple thermal evaporation in ambient air was used for forming TeO$_2$ nanowires. A modified gas evaporation method using vacuum evaporator, which rather easily provides a high raw material temperature and well-controlled atmosphere, was used for forming SnO$_2$ nanowires. In these methods, thin nanowires could be formed by adjusting both the atmosphere and heating temperature of raw materials.

A sensor made of SnO$_2$ nanowires formed by a vapour transport method showed a high sensitivity at a low temperature when doped with Pd, similarly to conventional SnO$_2$ sensors. It was found that a nanowire sensor indicated quicker response and recovery to H$_2$ than sputtered-film sensor, although the sensitivity was lower than sputtered film. Sensors made of SnO$_2$ nanowires and microwires formed by modified gas evaporation were superior to a sensor made of nanoparticles in sensitivity to NO$_2$, despite the smaller surface-to-volume ratio than nanparticles in the case of microwires. These sensors were also superior to the nanoparticle sensor in response and recovery speed to NO$_2$. In addition, a sensor with a gap length shorter than the length of nanowires was confirmed to be superior to sensors with longer gap length in sensitivity as well as response and recovery speed,

indicating the importance of the interface between the electrode and nanowires. As for WO_3 nanowire sensors, the sensitivity to NO_2 was confirmed to increase as the diameter of the nanowires decreased.

Ga_2O_3 nanowire sensor showed a sufficient sensitivity and reversible behaviour at relatively low temperature of 100-300°C. TeO_2 nanowires were first formed and evaluated as a gas sensing material. The sensor indicated p-type semiconductor character of TeO_2 nanowires, showing increase and decrease in resistance upon exposure to reducing gases (NH_3 and H_2S) and oxidizing gas (NO_2), respectively.

5. Acknowledgements

6. References

Akiyama, M.; Tamaki, J.; Miura, N. & Yamazoe, N. (1991). Tungsten oxide-based semiconductor sensor highly sensitive to NO and NO_2. *Chem. Lett.* 20, 9, (1991) 1611-1614, ISSN: 1348-0715 (print) , 0366-7022 (online).

Babana, C.; Toyodac, Y. & Ogita, M. (2005). Oxygen sensing at high temperatures using Ga_2O_3 films. *Thin Solid Films,* 484, (July 2005) 369-373, ISSN: 0040-6090.

Binet, L. & Gourier, D. (1998). Origin of the blue luminescence of β-Ga_2O_3. *J. Phys. Chem. Solids*, 59, (August 1998) 1241-1249, ISSN: 0022-3697.

Boudart, M. (1999). On the nature of spilt-over hydrogen. *J. Mol. Catal. A-Chem.*, 138, 2-3, (February 1999) 319-321, ISSN: 1381-1169.

Bowker, M.; Bowker, L.J.; Bennett, R.A.; Stone, P. & Ramirez-Cuesta, A. (2000). In consideration of precursor states, spillover and Boudart's 'collection zone' and of their role in catalytic processes. *J. Mol. Catal. A-Chem.*, 163, 1-2, (December 2000) 221-232, ISSN: 1381-1169.

Cao, B.; Chen, J.; Tang, X.J. & Zhou, W.L. (2009). Growth of monoclinic WO_3 nanowire array for highly sensitive NO_2 detection . *J. Mater. Chem.*, 19, 16, (2009) 2323-2327, ISSN: 0959-9428.

Chen, Y.Q.; Cui, X.F.; Zhang, K.; Pan, D.Y.; Zhang, S.Y.; Wang, B.; Hou, J.G. (2003). Bulk-quantity synthesis and self-catalytic VLS growth of SnO_2 nanowires by lower-temperature evaporation. Bulkquantity, *Chem. Phys. Lett.*, 369, (February 2003) 16-20, ISSN: 0009-2614.

Choi, H.G.; Jung, Y.H. & Kim, D.K. (2005). Solvothermal Synthesis of Tungsten Oxide Nanorod/Nanowire/Nanosheet. *J. Am. Ceram. Soc.*, 88, 6, (June 2005) 1684-1686, ISSN: 0002-7820.

Chung, Y.K.; Kim, M.H.; Um, W.S.; Lee, H.S.; Song, J.K.; Choi, S.C.; Yi, K.M.; Lee, M.J. & Chung, K.W. (1999). Gas sensing properties of WO_3 thick film for NO_2 gas dependent on process condition. *Sens. Actuator B-Chem.*, 60, (November 1999) 49-56, ISSN: 0925-4005.

Doi, K.; Sasaki, T. & Hijikata, K. (1975). Electrical properties of TeO_2. *Bull. Chem. Soc. Jap.*, 48, 1, (1975) 144-146.

Fleischer, M.; Giber, J. & Meixner, H. (1992). H_2-induced changes in electrical conductance of β-Ga_2O_3 thin-film systems. *Appl. Phys. A*, 54, 6, (1992) 560-566, ISSN: 0947-8396 (print), 1432-0630 (online).

Francioso, L.; Forleo, A.; Capone, S.; Epifani, M.; Taurino, A.M. & Siciliano, P. (2006). Nanostructured In_2O_3–SnO_2 sol–gel thin film as material for NO_2 detection. *Sens. Actuator B-Chem.*, 114, (April 2006) 646-655, ISSN: 0925-4005.

Hartmann, E. & Kovacs, L. (1982). Electrical conductivity of paratellurite (TeO_2) crystals. *Phys. Status Solidi. A*, 74, (Novembre 1982) 59-64, ISSN: 1862-6319 (online).

Heiland, G. (1982). Homogeneous semiconducting gas sensors. *Sens. Actuator.*, 2, (1982) 343-361.

Hernandez-Ramirez, F.; Tarancon, A.; Casals, O.; Arbiol, J.; Romano-Rodriguez, A. & Morante, J.R. (2007). High response and stability in CO and humidity measures using a single SnO_2 nanowire. *Sens. Actuator B-Chem.*, 121, (January 2007) 3-17, ISSN: 0925-4005.

Hong, K.Q.; Xie, M.H. & Wu, H.S. (2006). Tungsten oxide nanowires synthesized by a catalyst-free method at low temperature. *Nanotechnology*, 17, 19, (October 2006) 4830-4833, ISSN: 0957-4484.

Jain, H. & Nowick, A.S. (1981). Electrical conduction in paratellurite (TeO_2) crystals. *Phys. Status Solidi. A*, 67, (October 1981) 701-707, ISSN : 1862-6319 (online).

Jain, D.K. & Garg, J.C. (1979). Field-assisted conduction mechanism in tellurium dioxide films. *Indian J. Pure Appl. Phys.*, 17, 10, (1979) 642-645, ISSN: 0019-5596.

Jang, H.S.; Kang, S.O. & Kim, Y.I. (2006). Enhancement of field emission of SnO_2 nanowires film by exposure of hydrogen gas. *Solid State Commun.*, 140, (December 2006) 495-499, ISSN: 0925-4005.

Jin, C.J.; Yamazaki, T.; Shirai, Y. Yoshizawa, T.; Kikuta, T.; Nakatani, N. & Takeda, H. (2005). Dependence of NO_2 gas sensitivity of WO_3 sputtered films on film density. *Thin Solid Films*, 474, (March 2005) 255-260, ISSN: 0040-6090.

Kaito, C.; Fujita, K.; Shibahara, H. & Shiojiri, M. (1977). Electron microscopic study of metal oxide smoke particles prepared by burning metals in Ar– O_2 gas. *Jpn. J. Appl. Phys.*, 16, (May 1977) 697-704, ISSN: 0021-4922 (print), 1347-4067 (online) .

Kimoto, K.; Kamiya, Y. & Nonoyama, R. (1963). An electron microscope study on fine metal particles prepared by evaporation in argon gas at low Pressure. *Jpn. J. Appl. Phys.*, 2, (November 1963) 702-713, ISSN: 0021-4922 (print), 1347-4067 (online).

Kolmakov, A.; Klenov, D.O.; Lilach, Y.; Stemmer, S. & Moskovits, M. (2005). Enhanced gas sensing by individual SnO_2 nanowires and nanobelts functionalized with Pd catalyst particles. *Nano Lett.*, 5, 4, (April 2005) 667-773, ISSN: 1530-6984.

Korotcenkov, G.; Brinzari, V.; Schwank, J. & Cerneavschi, A. (2002). Possibilities of aerosol technology for deposition of SnO_2-based films with improved gas sensing characteristics. *Mater. Sci. Eng. C*, 19, (January 2002) 73-77, ISSN: 0928-4931.

Kumar, V.; Sen, S.; Muthe, K.P.; Gaur, N.K.; Gupta, S.K. & Yakhmi, J.V. (2009). Copper doped SnO_2 nanowires as highly sensitive H_2S gas sensor. *Sens. Actuator B-Chem.*, 138, (May 2009) 587-590, ISSN: 0925-4005.

Leblanc, E.; Perier-Camby, L ; Thomas, G ; Gibert, R ; Primet, M. & Gelin, P. (2000). NO_x adsorption onto dehydroxylated or hydroxylated tin dioxide surface. Application to SnO_2-based sensors, *Sens. Actuator B-Chem.*, 62, (January 2000) 67–72, ISSN: 0925-4005.

Liu, Z.; Yamazaki, T.; Shen, Y.; Kikuta, T.; Nakatani, N. & Kawabata, T. (2007). Room temperature gas sensing of p-type TeO_2 nanowires. *Appl. Phys. Lett.*, 90, 17, (April 2007) 173119, ISSN: 0003-6951.

Liu, Z.; Yamazaki, T.; Shen, Y.; Kikuta, T. & Nakatani, N. (2008). Synthesis and characterization of TeO_2 Nanowires. *Jpn. J. Appl. Phys.*, 47, 1, (January 2008) 771-774, ISSN: 0021-4922 (print), 1347-4067 (online).

Liu, Z.; Yamazaki, T.; Shen, Y.; Kikuta, T.; Nakatani, N. & Li, Y. (2008). O_2 and CO sensing of Ga_2O_3 multiple nanowire gas sensors. *Sens. Actuator B-Chem.*, 129, (February 2008) 666-670, ISSN: 0925-4005.

Mazeina, L.; Bermudez, V.M.; Perkins, F.K.; Arnold, S.P. & Prokes, S.M. (2010). Interaction of functionalized Ga_2O_3 NW-based room temperature gas sensors with different hydrocarbons. *Sens. Actuator B-Chem.*, 151, (November 2010) 114-120, ISSN: 0925-4005.

Polleux, J.; Gurlo, A.; Barsan, N.; Weimar, U.; Antonietti, M. & Niederberger, M. (2006). Template-free synthesis and assembly of single-crystalline tungsten oxide nanowires and their gas-sensing properties. *Angew. Chem. Int. Ed.*, 45, 2, (2006) 261-265, ISSN: 1433-7851.

Ponzoni, A.; Comini, E.; Sberveglieri, G.; Zhou, J.; Deng, S.Z.; Xu, N.S.; Ding, Y. & Wang, Z.L. (2006). Ultrasensitive and highly selective gas sensors using three-dimensional tungsten oxide nanowire networks. *Appl. Phys. Lett.*, 88, 20, (May 2006) 203101, ISSN: 0003-6951.

Rout, C.S.; Ganesh, K.; Govindaraj, A. & Rao, C.N.R. (2006). Sensors for the nitrogen oxides, NO_2, NO and N_2O, based on In_2O_3 and WO_3 nanowires. *Appl. Phys. A*, 85, (Novembre 2006) 241-246, ISSN: 0947-8396 (print), 1432-0630 (online).

Ruhland, B.; Becker, T. & Müller, G. (1998). Gas-kinetic interactions of nitrous oxides with SnO_2 surfaces. *Sens. Actuator B-Chem.*, 50, (July 1998) 85-94, ISSN: 0925-4005.

Schwebel, T.; Fleischer, M.; Meixner, H. & Kohl, C.D. (1998). CO-sensor for domestic use based on high temperature stable Ga_2O_3 thin films. *Sens. Actuator B-Chem.*, 49, 1-2, (June 1998) 46-51 ISSN: 0925-4005.

Schwebel, T.; Fleischer, M. & Meixner, H. (2000). A selective, temperature compensated O_2 sensor based on Ga_2O_3 thin films. *Sens. Actuator B-Chem.*, 65, (June 2000) 176-180, ISSN: 0925-4005.

Sergent, N.; Epifani, M; Comini, E; Faglia, G & Pagnier, T. (2007). Interactions of nanocrystalline tin oxide powder with NO_2: A Raman spectroscopic study, *Sens. Actuator B-Chem.*, 126, (Septembre 2007) 1–5, ISSN: 0925-4005.

Shen, Y.; Yamazaki, T.; Liu, Z.; Meng, D.; Kikuta, T.; Nakatani, N.; Saito, M. & Mori, M. (2009). Microstructure and H_2 gas sensing properties of undoped and Pd-doped SnO_2 nanowires. *Sens. Actuator B-Chem.*, 135, (January 2009) 524-529, ISSN : 0925-4005.

Shen, Y.; Yamazaki, T.; Liu, Z.; Meng, D.; Kikuta, T. (2009). Hydrogen sensors made of undoped and Pt-doped SnO_2 nanowires. *J. All. Comp.*, 488, (Novembre 2009) L21-L25, ISSN: 0925-8388.

Shimizu, Y.; Hyodo, T. & Egashira, M. (2007). H_2 sensing performance of anodically oxidized TiO_2 thin films equipped with Pd electrode. *Sens. Actuator B-Chem.*, 121, (January 2007) 219-230, ISSN: 0925-4005.

Tamaki, J.; Nagaishi, M.; Teraoka, Y.; Miura, N. & Yamazoe, N. (1989). Adsorption behavior of CO and interfering gases on SnO₂. *Surf. Sci.*, 221, (Octobre1989) 183-196, ISSN: 00396028.

Tamaki, J.; Miyaji, A.; Makinodan, J.; Ogura, S.; & Konishi S. (2005). Effect of micro-gap electrode on detection of dilute NO₂ using WO₃ thin film microsensors. *Sens. Actuator B-Chem.*, 108, (July 2005) 202-206, ISSN: 0925-4005.

Tamaki, J.; Hashishin, T.; Uno, Y.; Dao,D.V.; & Sugiyama, S. (2008). Ultrahigh-sensitive WO3 nanosensor with interdigitated Au nano-electrode for NO₂ detection. *Sens. Actuator B-Chem.*, 132, (May 2008) 234-238, ISSN: 0925-4005.

Tsang, S.C.; Bulpitt, C.D.A.; Mitvhell, P.C.H. & Ramirez-Cuesta, A.J. (2001). Some new insights into the sensing mechanism of palladium promoted tin (IV) oxide sensor. *J. Phys. Chem. B.*, 105, (June 2001) 5737-5742, ISSN: 1520-6106.

Yamazoe, N.; Kurokawa, K. & Seiyama, T. (1983). Effects of additives on semiconductor gas sensors. *Sens. Actuator* 4, (1983) 283-289.

Wang, J.X.; Liu, D.F.; Yan, X.Q.; Yuan, H.J.; Ci, L.J.; Zhou, Z.P.; Gao, Y.; Song, L.; Liu, L.F.; Zhou, W.Y.; Wang, G. & Xie, S.S. (2004). Growth of SnO₂ nanowires with uniform branched structures. *Solid State Commun.*, 130, (April 2004) 89-94, ISSN: 0038-1098.

Windischmann, H. & Mark, P. (1979). A model for the operation of a thin-film SnOx conductance-modulation carbon monoxide sensor. *J. Electrochem. Soc.*, 126, (April 1979) 627-633, ISSN: 0013-4651 (print), 1945-7111 (online) .
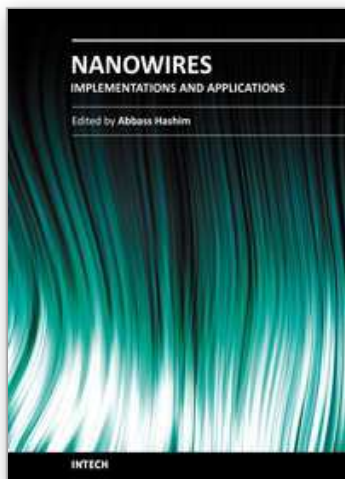
Nanowires - Implementations and Applications
Edited by Dr. Abbass Hashim

ISBN 978-953-307-318-7
Hard cover, 538 pages
Publisher InTech
Published online 18, July, 2011
Published in print edition July, 2011

This potentially unique work offers various approaches on the implementation of nanowires. As it is widely known, nanotechnology presents the control of matter at the nanoscale and nanodimensions within few nanometers, whereas this exclusive phenomenon enables us to determine novel applications. This book presents an overview of recent and current nanowire application and implementation research worldwide. We examine methods of nanowire synthesis, types of materials used, and applications associated with nanowire research. Wide surveys of global activities in nanowire research are presented, as well.

How to reference
In order to correctly reference this scholarly work, feel free to copy and paste the following:

Yamazaki (2011). Formation of Oxide Nanowires by Thermal Evaporation and Their Application to Gas Sensors, Nanowires - Implementations and Applications, Dr. Abbass Hashim (Ed.), ISBN: 978-953-307-318-7, InTech, Available from: http://www.intechopen.com/books/nanowires-implementations-and-applications/formation-of-oxide-nanowires-by-thermal-evaporation-and-their-application-to-gas-sensors

INTECH
open science | open minds